Experimental Analysis of the Near Wake from a Ducted Thruster at True and Near Bollard Pull Conditions Using Stereo Particle Image Velocimetry (SPIV)

S. El Lababidy

N. Bose

Memorial University of Newfoundland (MUN), Canada

P. Liu
Institute for Ocean Technology (IOT), Canada

D. Walker
Oceanic Consulting Cooperation, Canada

F. Di Felice
Italian Ship Model Basin (INSEAN), Italy

Thrusters working at low advance coefficients are employed in a wide range of offshore and marine applications on Floating, Production, Storage, and Offloading (FPSO) systems; shuttle tankers; tug boats; and mobile offshore units. Therefore, an understanding of the flow around the thrusters is of great practical interest. Despite this interest, there is lack of knowledge in the description of the hydrodynamic characteristics of a ducted thruster's wake at bollard pull and low advance coefficient values. This work was aimed at providing detailed data about the hydrodynamic characteristics of a Dynamic Positioning (DP) thruster near wake flow at different low advance coefficient values. Wake measurements were made during cavitation tunnel tests carried out on a ducted propeller model at the Italian Ship Model Basin (INSEAN), Rome, Italy. Through these experiments, the DP thruster near wake velocity components at different downstream axial planes, up to 1.5 diameters downstream, were obtained using a Stereoscopic Particle Image Velocimetry (SPIV) system. These experiments were carried out at different advance coefficient (J) values [bollard pull (J=0), J=0.4 and J=0.45].
[DOI: 10.1115/1.1951770]

Introduction

Over the past few years, application of Dynamic Positioning (DP) systems has increased in the offshore oil and gas industry. As operations move into more hostile and deeper waters, the need for DP systems has become almost mandatory. There are different types of thrusters used in DP systems, but the majority are ducted; steerable over 360 deg and mounted below the hull; or placed in tunnels crossing the hull from one side to the other.

An accelerating duct surrounding a propeller is used to improve propulsive performance of heavily loaded propellers. The experimental work of Luisa Stipa and later Kort (1934) showed the advantages that can be obtained by application of a nozzle in increasing the propulsive performance of ships with heavy loaded propellers (tugs, push boats, supply vessels, trawlers, and tankers).

DP systems have been available since the early 1960's, but they have come into much more common usage since offshore oil and gas exploration and production moved into deep waters. A historical review of the application and of different types of DP systems is provided by Morgan [1]. However, there is little research on the hydrodynamic characteristics of the flow around ducted DP thrusters at low advance coefficient values. The flow in the wake of a DP thruster involves several complex features: Transition zones, turbulence, presence of vortical structures, deformation, effects of waves and currents, vortex rollup and break down, shear layers, etc. These do not easily allow a complete evaluation of the flow features. However, experimental measurements become partly feasible through the introduction of nonintrusive laser techniques (laser Doppler velocimetry LDV and particle image velocimetry PIV). LDV is a single point measurement technique which has been widely used to evaluate complex flow fields such as propeller flows [2–9]. However, as with any experimental technique, LDV has some limitations:

- As a single point measurement technique, it cannot give an overall picture of the characteristics of large coherent structures which are generally encountered with complex and separated flows.
- The fixed location and time-averaged nature of the LDV technique can induce significant errors in the measurement of the intensity of unsteady vortical structures.
- It is a time consuming technique, as multiple measurements must be taken to construct a whole velocity field. This leads to increased cost of experiments and difficulties in the investigation of unsteady flows.

A dense grid of LDV measurements is required in order to resolve the flow structure during a propeller revolution in a nonuniform inflow [10]. The PIV technique, that can take simultaneous measurements over a given plane in the fluid, offers many advantages over the LDV technique. So, experimental measurements can be fast and easily conducted by acquiring images at each angular position of a propeller blade [11]. Since the initiation of PIV techniques, significant progress and improvements to the system have been made to broaden its range of application, increasing the capability and reliability of the measurement approach. Nowadays, the PIV technique is considered to be a powerful whole field measurement technique.

Stereoscopic PIV is an obvious measuring technique for complex propeller flow fields. It allows the construction of the three components of velocity fields by using two cameras to view the flow from two perspectives. The two images at a point in the flow are combined to yield a three-dimensional velocity vector field. By combining the vector fields from the two cameras, the three-dimensional velocity field over a plane is computed [11].

The operation of DP thrusters in the bollard pull condition adds

Contributed by the OOAE Division for publication in the JOURNAL OF OFFSHORE MECHANICS AND ARCTIC ENGINEERING. Manuscript received: August 26, 2004. Final revision: March 3, 2005. Associate Editor: Solomon Yim.

Table 1 Ducted propeller model and model nozzle particulars [14]

Main Particulars	Propeller	Model
Diameter	3.0 m	0.2 m
Number of Blades	4	
Hub to Propeller Diameter Ratio	0.367	
Expanded Area Ratio	0.604	
Nozzle Model Particulars		
Length	0.100 m	
Inside Diameter	0.202 m	
Nozzle Contraction Ratio	1.2223	

additional complexity to the wake, where the propeller is heavily loaded with very high propeller induced velocities. The blade sections are at a high angle of attack, with large radial flow, large section drag coefficient and very strong tip and hub vortices [12]. Generally, the limitations of cavitation tunnels do not enable measurements to be performed at a true bollard pull condition. The first true bollard pull ($J=0$) DP thruster wake survey was presented by El Lababidy et al. [13]. In that work, a comparison between the hydrodynamic characteristics of the same DP thruster far wake evolution when operating with and without a nozzle at true bollard pull operating condition and at different downstream axial planes up to 15 diameters downstream in the INSEAN large cavitation tunnel was presented. The characteristics of the INSEAN large cavitation tunnel allowed the investigation to include the bollard pull condition.

Experimental Setup

Tests were done in the INSEAN large cavitation tunnel. This is a free surface tunnel with a test section of 10 m in length, 3.6 m in width and 2.25 m in depth. The maximum allowable water speed is 5.2 m/s.

Tests were carried out at a propeller pitch ratio (P/D) of 1.2 and at a propeller speed of 20 rps for $J=0$ and 15 rps for $J=0.4$ and 0.45. The propeller model was a ducted controllable pitch propeller. The principal dimensions and particulars of the propeller, the model and the nozzle are given in Table 1 below [14].

Measurements were performed using an underwater SPIV probe. Figure 1 shows the probe and the thruster installed in the test section. When completely assembled, the probe forms a streamlined torpedolike tube with an external diameter of 150 mm. The tube was rigidly linked to a bench through two hydrodynamically optimized struts. The whole system could be

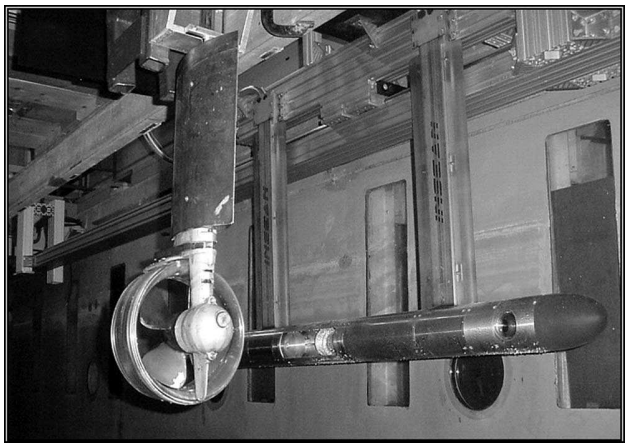

Fig. 1 DP thruster model and SPIV in the INSEAN large cavitation tunnel

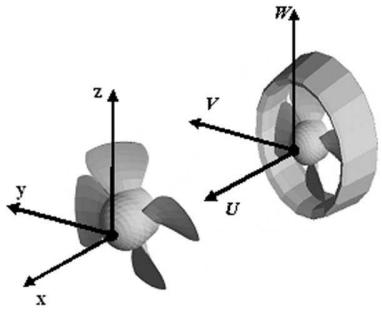

Fig. 2 Coordinate system. The mesh of the propeller and the nozzle were generated using PROPELLA [19]

traversed by a mechanism controlled by a PC to sweep the measurement plane up to $X/D=15$. The stereoscopic system consisted of two 2048×2048 pixels CCD cameras, with 12-bit resolution. The aperture, the focus and the Scheimpflug angle of the camera lenses were remotely controlled. The laser light was delivered to the underwater sheet optics through the struts and inside an articulated arm. Mirrors within the arm allowed the beam to be correctly aligned with the output optics. The laser optics consisted of a set of cylindrical and spherical lenses, which respectively expanded the beam into a sheet and focused it onto the measurement plane. The laser subsystem consisted of a pulse-doubled 15 Hz 200 mJ Nd-YAG laser rigidly attached to the probe support bench. The camera mirror sections were open to the water to avoid multimedia refractions and to minimize the optical aberrations through one single orthogonal water-air interface. More details on the underwater SPIV probe have been presented by Felli [15].

The overlapped imaged areas of the two cameras created a three-dimensional (3D) velocity field area of about 328 mm $\times$265 mm. The measurement errors for the adopted optical configuration have been previously assessed on a test bench [15] and are about 3% for the light sheet in plane components and about 2% for the out of plane components.

Coordinate System

A Cartesian (x,y,z) coordinate system was used. As shown in Fig. 2, the x axis is along the propeller shaft centerline and points downstream, the y axis is horizontal, and the z axis is vertical pointing upwards. As shown in Fig. 2 the longitudinal velocity is U and the cross-flow velocity components are V and W.

The wake velocity was initially analyzed by constructing the instantaneous 3D velocity vector field for each plane (129 images/plane) from the combination of the two-dimensional (2D) encoded velocity vector fields of the left and right camera. Then the mean 3D velocity field was constructed for each plane by averaging the summation of the instantaneous 3D vector files for each plane over 129.

Measurement Uncertainty

The technique used for the stereo reconstruction was the method described by Solof [16] and a detailed analysis of the errors was presented by Prasad [17].

The uncertainty of velocity measurements from each single camera is mainly due to the error in the particle displacement evaluation, which can be normally considered to be around 1/10 to 1/20 of a pixel for the image analysis and subpixel interpolation algorithms [18]. This was equivalent to approximately 3 cm/s in terms of velocity for the flow speeds considered here. This error is present in the measurement of the instantaneous flow field seen by each camera, but with the stereo reconstruction the error increases and is up to 10 cm/s for the longitudinal velocity component.

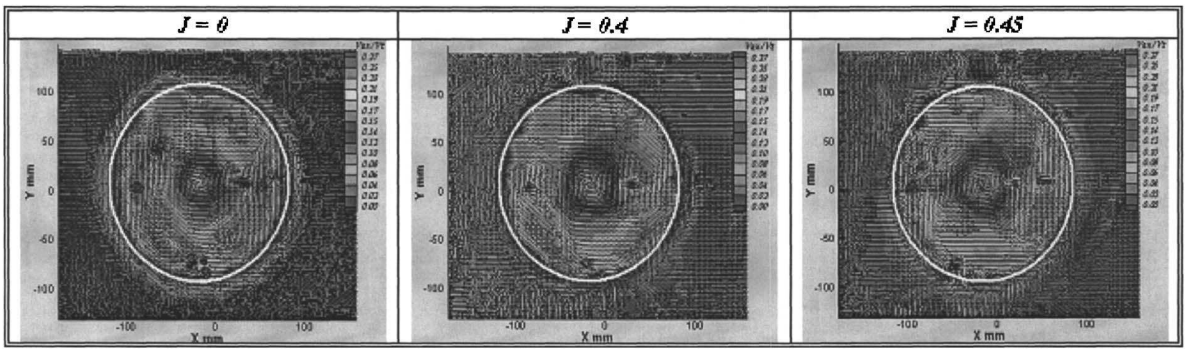

Fig. 3 Circumferential variation of velocity components around the ducted DP thruster at different J at $X/D=0.4$

This relatively large error is a typical value for a SPIV measurement and depends on many factors such as the optical configuration (angle between the cameras), optical aberrations, number of dots in the calibration target, number of planes used in the calibration, etc. The errors due to light reflections from the hub and from the blade edges and the nozzle were also important in flow field regions mapped in proximity to reflection spots.

The accuracy of the mean velocity field depends upon the number of acquired samples and upon the shape of the velocity probability distribution function. By using the Student t-distribution (for which the confidence interval for 95%, is $\pm 1.96^{*}\mathrm{RMS}/\sqrt{(N-1)}$, with $N=129$), it is possible to estimate the uncertainty in a velocity component to be about 1/6 of the measured root-mean squared (RMS) velocity.

Near Wake Characteristics

The ducted DP thruster near wake velocities were analyzed experimentally using SPIV at six downstream transverse planes (0.3, 0.4, 0.5, 0.75, 1.0, and 1.5 D) and at three different advance coefficient values ($J=0$, $J=0.4$, and $J=0.45$) in order to show the characteristics of the flow in this region.

All the results presented were obtained by phase averaging the measurements for a blade position having the trailing edge at the 12 o'clock position.

Velocity Field Characteristics Around the Ducted Propeller. Figure 3 shows the distribution of the normalized propeller wake velocity components, at the 0.4 D downstream axial position. Re-

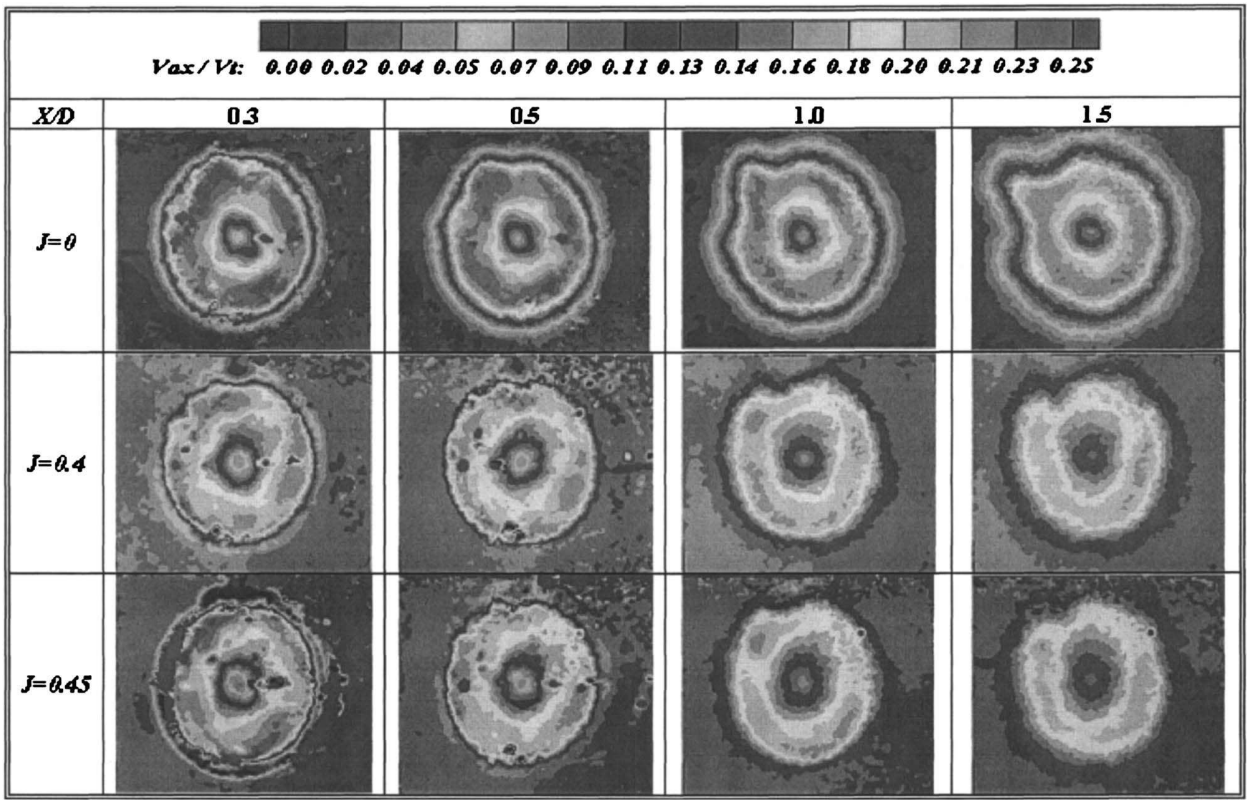

Fig. 4 Ducted DP thruster near wake velocity components evolution at different J

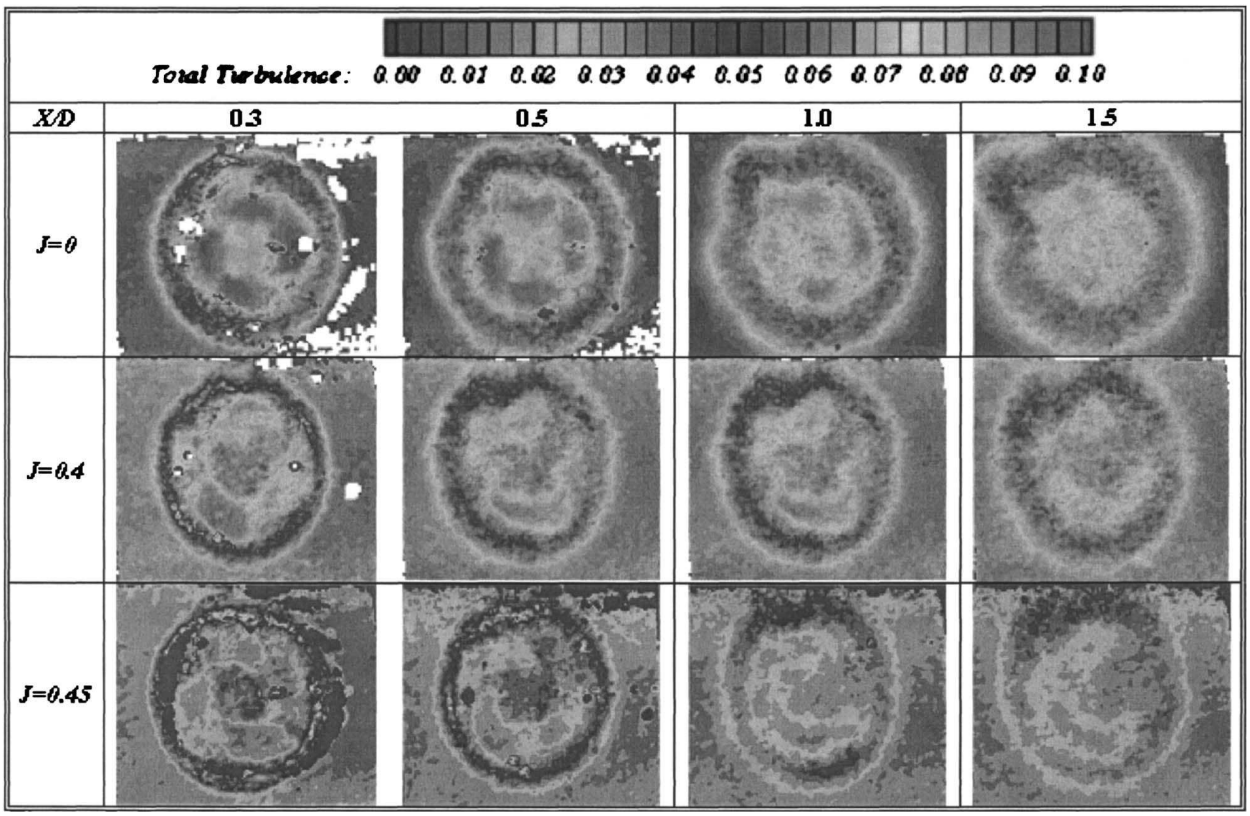

Fig. 5 Ducted DP thruster near wake total turbulence distribution at different *J*

sults are plotted for the ducted DP thruster at the bollard pull condition ($J=0$), $J=0.4$ and $J=0.45$. Wake velocity components were normalized by the propeller total flow velocity ($V_t=V_A+\omega r$). The results indicate some common features between the distributions of the flow velocity components among the three advance coefficients. The distribution of the axial velocity shows low values near the hub increasing radially outwards to reach a maximum value at a radial position around $r/R=0.6-0.8$. Some deformation occurs due to the high effect of the strut wake, which disturbs the inflow to the propeller.

Figure 3 also shows that the results at the bollard pull condition have higher axial and cross flow velocity components than the results at $J=0.4$ and $J=0.45$. Moreover, Fig. 3 indicates that there is a reduction in the axial and cross flow velocity components as advance coefficient increases. This is due to the reduction in the propeller blades' load as a result of increasing advance coefficient value.

Longitudinal Wake Evolution. Figure 4 shows the near wake distribution of the ducted DP thruster mean normalized axial velocity component at $X/D=0.3$, 0.5, 1.0, 1.5, and at different advance coefficient values. The evolution along the longitudinal axis of the axial velocity component shows that:

- the wake contraction between the first two planes, which are very close to each other and to the propeller plane, causes some axial acceleration which is indicated by the higher axial velocity achieved in the second measurement plane.
- a reduction in the longitudinal flow velocity starts beyond the second measurement plane ($X/D=0.5$).
- the beginning of the slipstream broadening is about one diameter from the propeller disk.

The near wake evaluation of the mean axial flow velocity shows that there is an increase in the axial velocity within the slipstream of the propeller as the advance coefficient is decreased (propeller load increases). It is also noted that the contraction of the propeller slipstream behind the propeller is higher at $J=0$ than $J=0.4$ and $J=0.45$.

The effect of the change in advance coefficient on the operation of the ducted DP thruster is also demonstrated by the distribution of the total flow turbulence shown in Fig. 5. The total flow turbulence, as presented by Eq. (1), has been defined as the nondimensional standard deviation of the velocity distribution at a given point by the propeller angular velocity.

$$\text{Total turbulence} = \frac{\sqrt{(\sigma U)^2 + (\sigma V)^2 + (\sigma W)^2}}{\omega D}, \qquad (1)$$

where, σ is the standard deviation of the velocity.

The distribution of the total flow turbulence shown in Fig. 5 indicates higher turbulence intensity level in the duct wake region than other wake regions. This implies that all the propeller blades are able to generate lift. El Lababidy et al. [13] present a comparison between the characteristics of the near and far wake of the DP thruster when operating with and without a nozzle at the bollard pull condition and at the same propeller operating speed. The results of that work indicate that measurements of open propeller have higher turbulence intensity in the propeller tip region than the measurements of ducted propeller at the same operating condition. This result implies that only the inner part of the open propeller blade is able to generate lift while the outer blade regions are stalled. Moreover, this result indicates the effect of the duct in accelerating the flow toward the propeller, increasing the effective advance ratio, reducing the thrust loading on the propeller blades and improving the propeller blade working conditions.

Also, the results presented by El Lababidy et al. [13] indicate that the wake of the ducted propeller persists further downstream

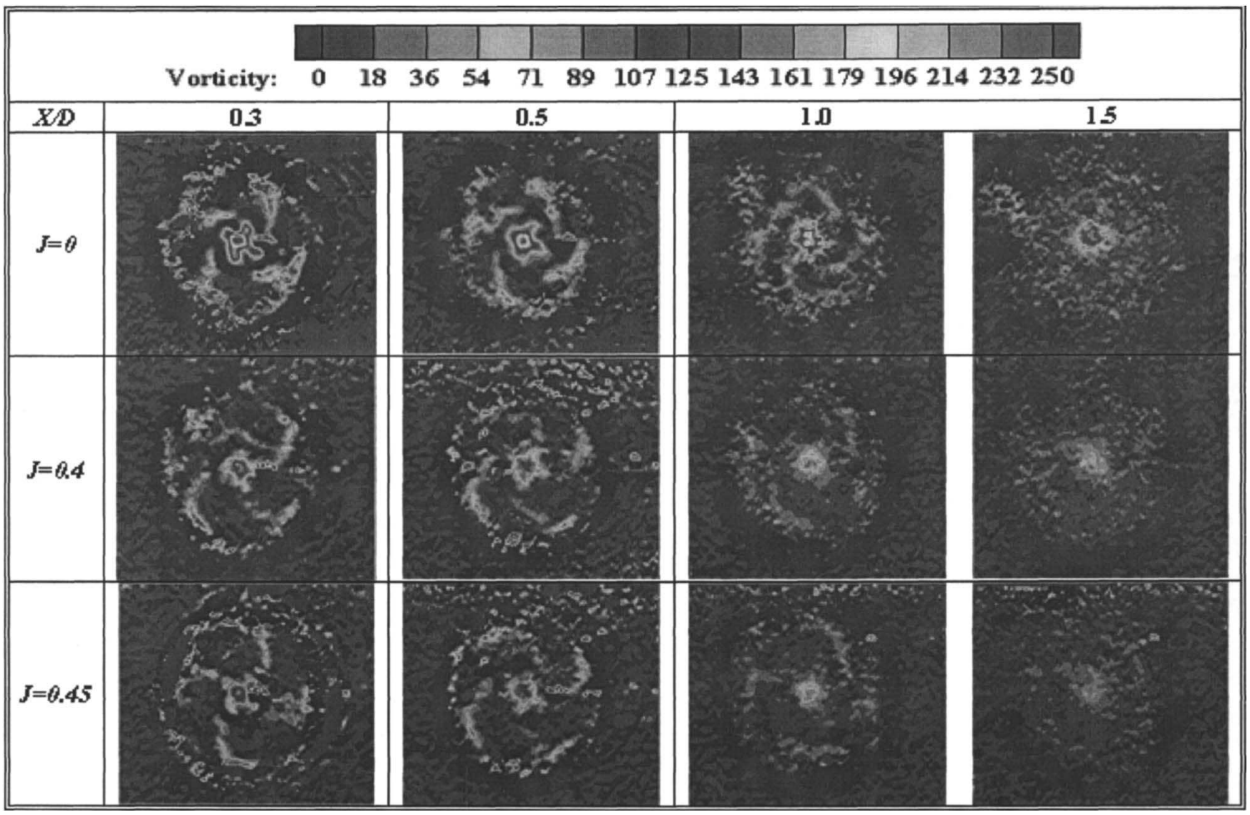

Fig. 6 Ducted DP thruster near wake vorticity distribution at different *J*

than that of the open propeller. Figure 4 indicates that the reduction and the fluctuation in the axial velocity among the measured axial planes when moving downstream from the propeller are reduced as J increases. Therefore, it is expected that the wake of the ducted DP thruster will persist further downstream as the advance coefficient increases. The rate of wake energy decay decreases as the advance coefficient increases.

Moreover, Fig. 5 shows that there is a reduction in the total flow turbulence around the ducted thruster as the advance coefficient and X/D increase.

The propeller blade wakes themselves could not be recognized from the mean flow velocity components and total flow turbulence distribution shown in Figs. 4 and 5, respectively. Figure 6 shows the vorticity distribution of the ducted DP thruster at different advance coefficient values and downstream axial positions. As shown in Fig. 6 the blade wake almost disappears within one diameter downstream, whereas a strong deformation, due to the higher axial velocity at the inner radius bends the blade wake. The maximum vorticity is found at the hub and propeller blade tip regions. The trailing vorticity, shed from the blade trailing edges, is easily identified and consists of two circular layers of opposite sign which overlap at about $r/R=0.7$, at the blade section of maximum loading. This result was also obtained by Felli et al. [11] and El Lababidy et al. [13].

The hub region has the strongest vortex structure of the propeller wake as shown in Fig. 6. This is due to the strong roll up process of the hub vortex due to the strong acceleration of the radial velocity component near the propeller hub. It is difficult to identify the tip vortices due to the high loading condition of the test. Figure 6 shows that there is a reduction in flow vorticity as X/D increases.

Measurements at bollard pull condition indicate higher vorticity at similar downstream axial positions than those at $J=0.4$ and $J=0.45$. Moreover, the decay of the hub vortices occurs in the near wake region of the measurements at $J=0.4$ and $J=0.45$, while measurements at $J=0$ indicate a high hub vortex region in the last near wake measuring plane ($X/D=1.5$).

Conclusion

The analysis of a ducted DP thruster wake when operating at the bollard pull ($J=0$) and low advance coefficient ($J=0.4$ and $J=0.45$) conditions in a large cavitation channel has been performed using a stereo-PIV system.

The analysis of the measurements of fluid flow velocity in the ducted thruster slipstream at different advance coefficient values indicates that as the advance coefficient increases, the propeller load is decreased and the magnitude of the axial velocity component and the thrust produced from the ducted propeller are reduced within the slipstream of the propeller. The analysis of the ducted DP thruster wake vorticity indicates a reduction in the wake vorticity as the propeller loading decreases (higher advance coefficient). Also, the results indicate that there is a rapid reduction of the vorticity as the distance from the propeller increases. This implies a high rate of vorticity dissipation and diffusion in the near wake region. Moreover, as expected the results indicate that the duct adds positive thrust to the propeller at the bollard pull condition. This thrust is reduced as advance coefficient increases due to the increase in the duct drag force.

From the experimental point of view, stereo-PIV shows a number of advantages compared with the well-assessed LDV technique. Considering the limited time usually available for these tests combined with the management and technical difficulties typical of operating a large testing facility, the PIV technique can provide results within a short period. The LDV technique requires up to three to four times more testing time to obtain the same information, which consequently translates into additional costs of facility occupancy. The measurement time is drastically reduced

with the stereo-PIV method, where the plane of measurement is mapped instantaneously and provides all three-velocity components in one single step. The LDV technique requires multiple measurements to scan the interrogation domain. In this sense, the PIV approach offers the freedom of extending wake survey to a larger number of areas of interest, with very limited setup changes. The major drawbacks of the PIV technique are a reduced accuracy with respect to the LDV technique and the huge quantity of information gathered. One must address the critical problem of storing, managing, and processing this information without compromising the test costs by extended data processing time.

Acknowledgments

We thank the Institute for Ocean Technology of the National Research Council Canada, Memorial University of Newfoundland, the Italian Ship Model Basin (INSEAN), Rome—Italy, and Petroleum Research Atlantic Canada for the financial support of this experimental work, and the Natural Sciences and Research Council, Canada, for the provision of a **PGS B** fellowship to the first author. This Project was undertaken and completed with a Grant and the financial assistance of Petroleum Research Atlantic Canada (PRAC). Thanks are due to Norsk Hydro Canada for their participation in the travel support for Said El Lababidy to visit INSEAN through a grant to Dr. Thormod Johansen, and to the INSEAN large cavitation tunnel technical staff, for their support and help during the experimental work.

Nomenclature

D = propeller diameter, m
J = advance coefficient, $J=V_A/(nD)$
n = angular speed of propeller shaft, rev/s
p = propeller pitch, m
r = propeller radius, m
V_A = velocity of advance, m/s
V_t = total flow velocity, m/s
w = propeller angular velocity, rad/s
X = axial downstream distance, m

Greek Symbols

ξ = flow vorticity, s^{-1}
σ = velocity standard deviation

References

[1] Morgan, M. J., (1978), *Dynamic positioning of offshore vessels*, PPC Books Division, Petroleum Pub. Co.
[2] Min, K. S., (1978), "Numerical and Experimental Methods for Prediction of field point velocities around propeller blades," Massachusetts Institute of Technology (MIT), Department of Ocean Engineering, Report No. 78-12.
[3] Kobayashi, S., (1982), "Propeller Wake Survey by LDV," *4th International Symposium on Application of Laser-Doppler Anemometry to Fluid Mechanics*.
[4] Cenedes, A., Accardo, L., and Milone, R., (1984), "Phase Sampling Techniques in the Analysis of Propeller Wake," *International Conference on Laser Anemometry Advances and Application*, Manchester UK.
[5] Hoshino, T., and Oshima, A., (1987), "Measurement of Around Propeller by Using 3-Component Laser Doppler Velocimeter," Mitsubishi Technical Review.
[6] Jessup, S. D., (1989), "An Experimental Investigation of Viscous aspects of Propeller Blade Flow," Ph.D. Thesis, The Catholic University of America, Washington D.C.
[7] Stella, A., Guj, G., Felice, F., and Di Elefante, M., (1998), "Propeller Wake Evaluation Analysis by LDV," *22nd Symposium on Naval Hydrodynamics*, Washington.
[8] Chesnack, C., and Jessup, S., (1998), "Experimental Characterisation of Propeller Tip Flow," *22nd Symposium on Naval Hydrodynamics*, Washington D.C.
[9] El Lababidy, S., Bose, N., and Liu, P., (2004a), "Evaluation of a Dynamic Positioning Thruster Wake using Laser Doppler Velocimetry," *23rd International Conference on Offshore Mechanics and Arctic Engineering*, Vancouver, British Columbia, Canada.
[10] Di Felice, F., Felli, M., and Ingenito, G., (2000), "Propeller Wake Analysis in Non Uniform Inflow by LDV," *Proceedings of the Propeller and Shafting Symposium*, Virginia Beach.
[11] Felli, M., Pereira, F., Calcagno, G., and Di Felice, F., (2002), "Application of Stereo-PIV: Propeller Wake Analysis in a Large Circulation Water Channel," *International Symposium of Application of Laser Anemometry to Fluid Mechanic*, Lisbon, Portugal.
[12] Jessup, S., Chesnakas, C., Fry, D., Donnelly, M., Black, S., and Park, J., (2004), "Propeller Performance at Extreme Off Design Conditions," *25th Symposium on Naval Hydrodynamics*, St. John's, NL, Canada.
[13] El Lababidy, S., Bose, N., Liu, P., Di Felice, F., Felli, M., and Pereira, F., (2004b), "Experimental Analysis of the Wake from a Dynamic Positioning Thruster," *25th Symposium on Naval Hydrodynamics*, St. John's, NL, Canada.
[14] Doucet, J. M., (1996), "Cavitation Erosion Experiments in Blocked Flow with Two Ice Class Propeller Models," Master Thesis, Faculty of Engineering and Applied Science, Memorial University of Newfoundland, Canada.
[15] Felli, M., (2003), "A versatile Fully Submersible Stereo-PIV Probe for Tow Tank Applications," *Fluid Measurements and Instrumentation Symposium*, Honolulu, Hawaii, USA.
[16] Solof, S. M., Adrian, R. J., and Liu, Z. C., (1997), "Distortion Compensation for Generalized Stereoscopic Particle Image Velocimetry," Meas. Sci. Technol., **8**.
[17] Prasad, A. K., (2000), "Stereoscopic Particle Image Velocimetry," Exp. Fluids, **29**.
[18] Raffel, M., Willert, C., and Kompenhans, J., (1998), *Particle Image Velocimetry*, Springer.
[19] Liu, P., (2002) "Design and Implementation for 3D unsteady CFD Data Visualization Using Object-Oriented MFC with OpenGL," Comput. Fluid Dyn. J., Vol. 11.
[20] Carlton, J. S., (1994), "*Marine Propellers and Propulsion*," Oxford, Butterworth-Heinemann, Toronto, Canada.
[21] El Lababidy, S., (2003), "Performance Tests of a Dynamic Positioning Thruster with and without Nozzle, IMD Cavitation Tunnel Tests with MV Robert LeMeur Propeller Model," OERC Report No. 2003-02, Memorial University of Newfoundland, Canada.